18,13

Laser-induced graphene and its modification with polypyrrole for increasing microsupercapacitor capacitance

© K.G. Mikheev, A.V. Syugaev, R.G. Zonov, D.L. Bulatov, G.M. Mikheev

Udmurt Federal Research Center, Ural Branch Russian Academy of Sciences, Izhevsk, Russia

E-mail: k.mikheev@udman.ru

Received November 18, 2022
Revised November 18, 2022
Accepted November 25, 2022

Laser-induced graphene (LIG) films were synthesized by line-by-line scanning of *cw* CO_2 laser focused radiation on the surface of industrial polyimide film as a result of pyrolysis of its near-surface layer. The structure of the synthesized film material is shown to be heterogeneous in thickness by Raman spectroscopy. The results of the study of the effect of the laser power and the distance between the lines on the specific electrical capacitance c of the synthesized material in aqueous solution of sulfuric acid are presented. It is shown that modification of LIG with polypyrrole (PPy) allows to increase c up to 60 mF/cm^2. PPy-modified LIG films were used to make a prototype of a flexible film microsupercapacitor with an area of 8 cm^2, using a gel electrolyte based on sulfuric acid and polyvinyl alcohol, with a 230 mF capacitance.

Keywords: laser-induced graphene, electric capacitance, polypyrrole, microsupercapacitor.

DOI: 10.21883/PSS.2023.02.55422.529

1. Introduction

Graphene having sp^2 carbon two-dimensional hexagonal lattice is one of the promising materials suitable to be used in electronics and photonics. According to [1–5], a wide range of various methods has been developed for graphene synthesis. However, all of them are labour consuming and require dedicated equipment. Therefore, alternative graphene synthesis methods and graphene-containing materials are continuously searched for.

Recently in [6], a simple method was offered for graphene film structure synthesis by means of polyimide film subsurface pyrolysis with line-by-line scanning of focused pulse-periodic CO_2 laser radiation. A film structure synthesized by this technique received the name „laser-induced graphene“ (LIG). The synthesis requires no special conditions. LIG may be obtained on a polyimide film surface in air or in any other atmosphere during quite a short time. Further multiple investigations have shown that LIG may be produced using various pulse-periodic and *cw* lasers operating on various wavelengths [7–13].

It has been found that LIG can be synthesized on the surface of other materials (various biodegradable and natural polymer materials) [14]. By now, it has been demonstrated that almost any carbon-containing material can be converted into LIG using laser pyrolysis [15]. It has been found that varying the laser pulse energy and the power density of pulse-periodic laser allows to control the synthesized LIG morphology [8]. The synthesized LIG parameters are also greatly influenced by the initial precursor, scanning rate and line spacing, with fixed focused laser beam diameter [16,17]. According to [18], multiple laser treatment results in apparent reduction in the number of LIG defects and significant increase in surface resistivity of the synthesized film material. Test environment impact on the LIG properties has been also studied [19]. In particular, LIG obtained in air and oxygen atmosphere has been found to be hydrophilic, and hydrophobic LIG may be obtained in hydrogen and argon atmosphere.

LIG is a multifunctional material whose applications are demonstrated in a wide range of devices [20]. LIG can be used to reduce friction [21], to produce microsupercapacitors, electrocatalysts (see [22]) and various sensors, e.g. humidity sensors [11,23] and strain sensors [24], bolometers [25], various biosensors [26,27] as well as quick-response photodetectors [28] based on photon-drag effect [29,30].

It is not possible to list the huge number of publications devoted to LIG investigations and applications herein. However, we should separately address potential applications of LIG as flexible electrodes for tiny supercapacitors, which are referred to as microsupercapacitors (MSC). MSC development is required to produce miscellaneous portable electronic devices [31–34]. LIG-based MSC are distinguished by their stability in multiple bending conditions which indicates that they are suitable for flexible electronics [22].

LIG-based MSC can be produced due to 3D porous structure with highly-developed surface and low resistivity. LIG layer thickness, pore size and distribution are essential for LIG-based MSC development. MSC made from LIG functions due to electrode-electrolyte interface charging, and its capacitance is limited by the double electrical layer capacitance and space charge capacitance. MSC

capacitance can be additionally increased by means of boron doping of LIG during pyrolysis of polyimide film containing boron acid [35]. Boron presence in LIG changes its electronic structure and surface properties, which results in about 3 times higher specific surface capacitance of LIG-based MSC compared with MSC formed from traditional non-doped LIG. It is also advantageous to increase LIG capacitance by means of modification with redox-active compounds, e.g. transition metal oxides and oxyhydroxides (MnO_2, FeOOH) and conductive polymers (polyaniline) [36]. It should be noted that the great majority of investigations of LIG-based MSC production were carried out on electrodes synthesized by pulse-periodic lasers. Meanwhile, we have recently shown that LIG surface synthesized by *cw* laser emission is characterized by higher homogeneity compared with LIG surface obtained using pulse-periodic laser [18]. Hence, it is interesting to study capacitance properties of MSC made from LIG electrodes synthesized by continuous CO_2 laser radiation.

The purpose of this study is to investigate the influence of *cw* CO_2 laser radiation power and line spacing on capacitance of LIG film structures and possibility of LIG modification using polypyrrole (PPy) — a conductive redox-active polymer — in order to make MSC of higher capacitance.

2. Experimental details

For the purpose of the experiments, LIG was synthesized on a 125 μm polyimide film surface by line-by-line scanning of focused *cw* CO_2 laser radiation with power P up to 40 W [16,18] (see Figure 1, *a*). Laser power was measured using PM100D with S425C-L (Thorlabs) sensing head. A lens with a focal length of 51 mm was used for radiation focusing. And the laser beam diameter on the film surface measured at $1/e^2$ was equal to 120 μm. LIG was synthesized at laser power $P = 1-8$ W and beam scanning rate $v = 220$ mm/s. This rate was chosen based on the results of preliminary study of the synthesized carbon material structure that had been carried out using Raman spectroscopy (see below and [18]). The minimum spacing between the adjacent lines Δ (spacing between the adjacent parallel lines along which the beam moves) was equal to 25 μm.

The synthesized film structures were studied using an optical and scanning-electron microscope (SEM), Termo Fisher Scientific Quattro S; X-ray photoelectron spectrometer (XPS), SPECS Surface Nano Analysis GmbH; and Raman spectrometer, HORIBA HR800.

Electrochemical properties of the synthesized LIG film structures were examined at room temperature in natural aeration conditions by a potentiodynamic method in two-electrode or three-electrode configurations using P-20X and P-45X potentiostats in 1 M H_2SO_4 aqueous solution. LIG sample dimensions were equal to 10×10 mm^2 with special 8×8 mm^2 bonding pads. For electrochemical measurements, a current collector was attached to the bonding pad using conducting adhesive, then the pad was thoroughly insulated by paraffin. In two-electrode configuration, two identical specimens were immersed into the acid solution in the same plane at a distance of 1 mm between the adjacent sides. In three-electrode configuration measurements, a cell with separated spaces was used. A silver chloride electrode was used as a reference electrode, and a platinum electrode was used as an auxiliary electrode. Potential sweep rate was 20 mV/s. Specific capacitance (mF/cm^2) was calculated by the quantity of charge flowing via the specimen relative to the geometric surface area and potential range.

PPy was electrochemically deposited onto the LIG surface from stagnant 0.1 M pyrrole solution at room temperature, 0.5 M sulfuric acid solutions was used as background electrolyte. Galvanostatic deposition at current density 1 mA/cm^2 was used. Since the current efficiency for pyrrole electropolymerization is close to 100%, the quantity of charge flowing via the specimen was used to calculate the weight of the electro-deposited PPy.

PPy-modified LIG films were used to make a capacitor mockup in the form of two 2×4 cm^2 parallel PPy-modified plate LIG electrodes separated with a polypropylene separator and coated with hydrogel. The hydrogel electrolyte was produced as follows. Solution containing 10 ml deionized water and 1.0 ml 98% sulfuric acid was mixed by shaking. 1.0 g 16/1 grade PVA (GOST 10779-78) was added to the solution. PVA was dissolved as follows: first — 4-hour swelling of accurately weighed 1.0 g PVA at room temperature, and then final dissolution with periodic stirring and permanent heating at 90−95°C. The obtained solutions were transparent and, when cooled down, formed a transparent gel on the surface. The hydrogel was uniformely applied to the modified LIG surface. For electrochemical measurements, copper strip conductors were attached to the capacitor electrodes using conducting adhesive.

3. Results and discussion

Findings of the synthesized film structure testing carried out using optical microscope and SEM, XPS and Raman spectrometers are described in detail in out earlier publications [16,18,28].

Typical SEM image of a LIG surface is shown in Figure 1, *b*. It can be seen that the film surface is porous and nonuniform. There are sloped and vertically oriented fragments in the form of thin petals. In general, the surface is mostly composed of porous foam material consisting of petals interconnected in a 3D matrix. Pore sizes can achieve several micrometers and petal width is about 100 nm.

Figure 1, *c* shows cross-sectional SEM image of LIG film structure synthesized at $\Delta = 25$ μm. The shown film cross section was obtained at right angle to the laser beam scan lines which are parallel to the y-axis of Cartesian coordinate system xyz (see Figure 1, *a*). The number of lines increased

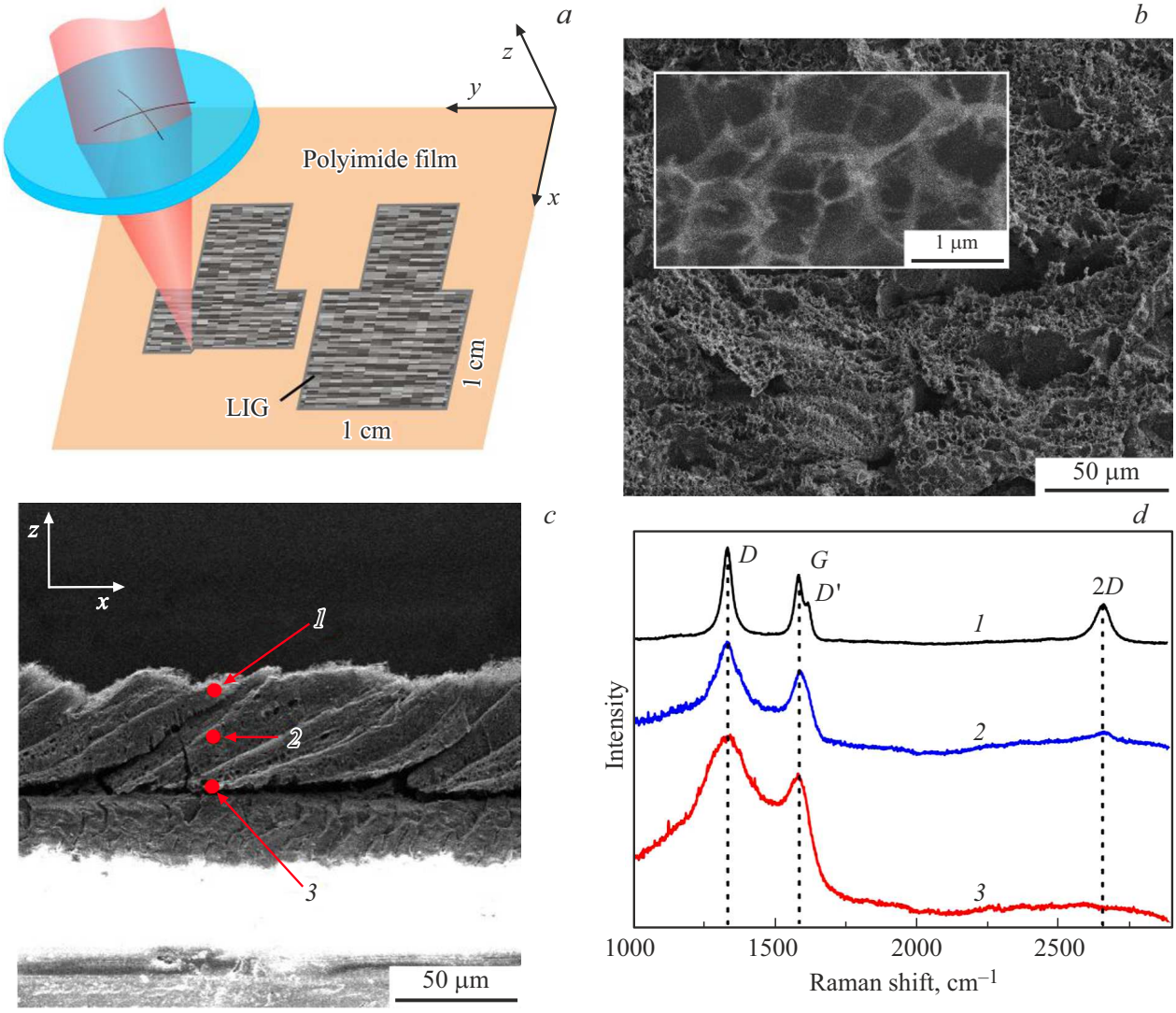

Figure 1. (*a*) Test set-up for laser synthesis of microsupercapacitor electrodes on a polyimide film surface; SEM images of (*b*) the LIG film structure surface and (*c*) its cross-section; Raman spectra recorded on (*1*) the LIG surface and (*2*) in points corresponding to the LIG film mid-thickness in depth and (*3*) LIG-polyimide film interface. *xyz* — is the Cartesian coordinate system. LIG was synthesized with laser beam scanning along the *y*-axis.

in *x*-direction, i.e. the film structure was synthesized in a plane parallel to plane *xy* in *x*-direction. The image shows that the LIG film structure with a thickness of about 50 μm has a pronounced interface with the polyimide film. It is apparent that the synthesized structure is lamellar with upper (free) sections of layers sloped in *x*-direction related to the *z*-axis. Each of these layers is synthesized by laser beam movement along the line parallel to the *y*-axis and the synthesized LIG layer slope in the *x*-direction is caused by the specificity of the synthesis, in which the film structure is formed in the *xy* plane in the *x*-axis direction free from carbon material.

Figure 1, *d* shows the Raman spectra recorded in three different points *1, 2, 3* on the *z*-axis (see Figure 1, *c*) that are located on a film surface, inside LIG (film mid-thickness), and at the LIG-polyimide film interface, respectively.

The Raman spectrum recorded on the film surface (see Figure 1, *d*, curve *1*) has four bands *D* (1329 cm^{-1}), *G* (1582 cm^{-1}), *D′* (1610 cm^{-1}) and 2*D* (2660 cm^{-1}) typical of LIG. Raman band *D* occurs due to defects in the hexagonal structure of sp^2 carbon atoms. It is not observed in Raman spectra of defect-free graphite and graphene [37]. *G*-band is associated with the longitudinal oscillation mode of carbon atoms. The figure shows that these bands do not overlap. According to the literature, the single-layer graphene spectrum is distinguished by intense 2*D*-band. It is fitted by one Lorenz curve with a half-width of 25 cm^{-1} while $I_{2D}/I_G > 1$, where I_{2D} and I_G are intensities of bands 2*D* and *G*, respectively [37]. Ferrari et al. [38] have shown that with the increase in the number of graphene layers, the 2*D*-band becomes wider and is described by several curves and its intensity becomes significantly lower

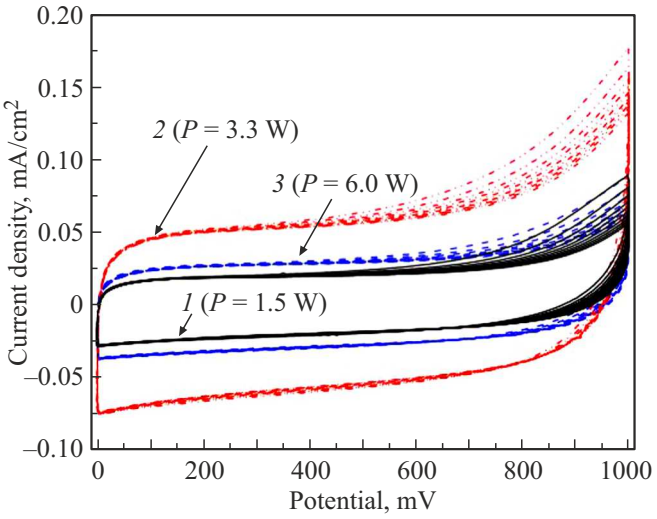

Figure 2. Cyclic voltammograms of LIG in 1 M H_2SO_4 solution at laser power $P =$ (*1*) 1.5 W, (*2*) 3.3 W and (*3*) 6 W. The curves were obtained for the two-electrode configuration with fixed $\Delta = 25\,\mu$m and $v = 220$ mm/s.

compared with the intensity of the *G*-band. In the recorded spectra, curve *1* also has the *D*′-band associated with the double resonance scattering process [39]. This band may be indicative of defects in graphene layers associated, for example, with nitrogen atoms which presence in LIG is confirmed by XPS data [25]. The spectrum decomposition on curve *1* shows that $I_{2D}/I_G \sim 0.5$, $I_D/I_G \sim 0.4$, where I_D — is intensity of the *D*-band. In this case, the width of 2*D* band that is described by one Lorenz curve does not exceed $\sim 45\,\text{cm}^{-1}$. According to multiples publications on LIG synthesis [22,40], all of these facts suggest that the synthesized material on the film surface is composed of multilayer graphene petals randomly oriented relative to each other.

In the Raman spectrum obtained in point *2* corresponding to the film mid-thickness in depth (see Figure 1, *c*), the *D* and *G*-bands are considerably wider and the intensity of the 2*D*-band is considerably lower than the corresponding data obtained on the LIG film surface. For this, $I_{2D}/I_G \sim 0.1$.

In the Raman spectrum recorded in point *3* corresponding to the LIG-polyimide film interface, the 2*D*-band does not occur at all and the *D* and *G*-bands almost merge each other. Such Raman spectrum is typical of amorphous carbon. All of these facts mean that the synthesized film structure has nonuniform thickness and the graphene-like structure of carbon is primarily formed in a near-surface layer of the synthesized film structure.

XPS tests have shown that there are various oxygen-containing and nitrogen-containing groups in the LIG near-surface layer (for details, see [18,25]). The presence of such groups makes the surface of the synthesized LIG film structures hydrophilic. The tests have shown that the synthesized LIG film structures are hydrophilic, which is important for aqueous electrolyte impregnation into LIG.

The experiments have shown that the measured capacitance of the synthesized specimens is greatly influenced by previous soaking in electrolyte. Measurements have shown that LIG specimen soaking in sulfuric acid during two days enables the capacitance to be increased by approximately a factor of 1.4 compared with the capacitance of a specimen without preliminary soaking. LIG soaking in electrolyte facilitates more complete penetration of the latter even in the finest pores throughout the film structure thickness. Increased area of phase interfaces in contact with the electrolyte results in increased specific capacitance of LIG.

Figure 2 shows voltammetry curves (10 cycles) of the LIG film structures synthesized with constant $\Delta = 25\,\mu$m and $v = 220$ mm/s, but with different incident radiation

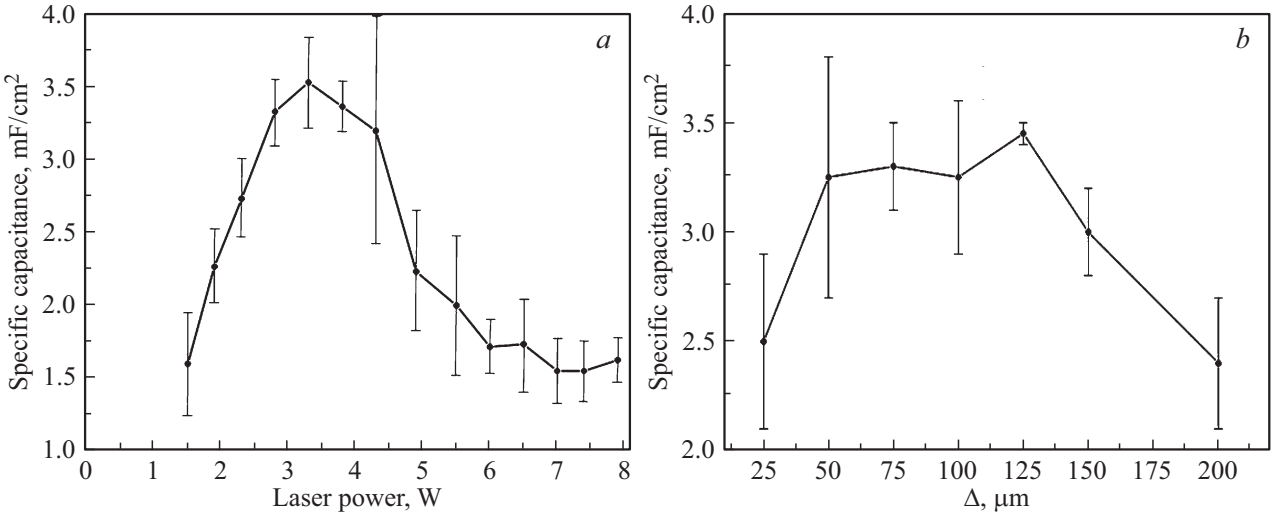

Figure 3. LIG film structure specific capacitance dependences on (*a*) laser power (with fixed $\Delta = 25\,\mu$m and (*b*) $v = 220$ mm/s) and spacing between adjacent lines Δ (with fixed laser power values $P = 4.3$ W and $v = 220$ mm/s).

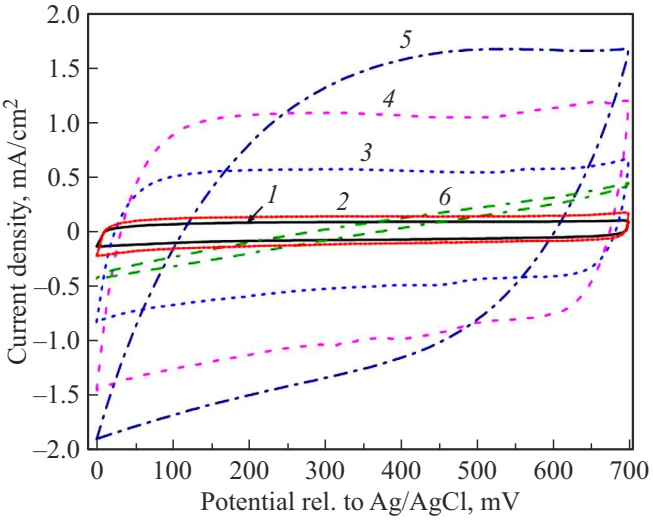

Figure 4. Stable cyclic voltammograms of LIG in H_2SO_4 aqueous solution according to the amount of deposited PPy: *1*–*6* — 0, 20, 100, 200, 350 and 800 μg/cm^2, respectively. The voltammograms were obtained for three-electrode configuration.

power values P. The shape of obtained cyclic voltammograms is close to rectangular. It can be clearly seen that the areas under voltammograms proportional to specific capacitance considerably depend on P. Figure 3, *a* shows LIG film structure specific capacitance dependence on radiation power. Specific capacitance depends on the laser power in a non-monotonic way. At low laser power, thin LIG film is formed, therefore specific capacitances are low. At high P values, high-energy plasma that occurs when laser radiation interacts with polyimide film during laser beam movement along the current line destroys the graphene layer which had formed earlier on the previous line. In these conditions, thin LIG films with low specific capacitances are formed. Thus, optimum laser power ($P \sim 3.5$ W) exists, where LIG film structure thickness and specific capacitance are maximum at fixed Δ and v.

Figure 3, *b* shows the measured specific capacitance dependence of LIG on Δ at fixed $P = 4.3$ W and $v = 220$ mm/s. The figure shows that for specimens obtained at $\Delta = 50-125\,\mu$m, spacing between lines has low influence on the film structure specific capacitance. However, with further increase of Δ, monotonous specific capacitance decrease is observed. This is an expected result, because when Δ are compared with the laser beam diameter, less than the whole surface of the scanned polyimide film is fully subjected to laser pyrolysis.

Figure 4 shows stabilized voltammograms of LIG specimen after PPy deposition in various amounts. Figure 5 shows the measured specific capacitance dependences calculated both per surface unit of the specimen and per weight unit of deposited PPy. The obtained dependences clearly show that PPy deposition results in considerable specific capacitance growth due to PPy participation in oxidation-reduction reactions, i.e. reversible transition of doped electron-deficient form PPy^+An^- into neutral non-doped form PPy^0:

$$[PPy^+An^-] + e \rightarrow PPy^0 + An^-,$$

where An — is anion. However, the capacitance ceases to increase with prolonged deposition. This result is caused by gradual reduction of pore diameter (i.e. reduction of active surface participating in oxidation-reduction reactions) and pore insulation with deposited polymer. At a certain deposition stage, accumulation of a bulk polymer phase starts. This phase is isolated from the electrolyte and is not involved in redox reactions. Accumulation of the inactive bulk phase is well seen by gradual reduction of specific capacitance based on the weight of deposited PPy during long-term deposition. Considerable capacitance drop at 800 μg/cm^2 corresponds to full occlusion of all LIG pores and formation of a „flat“ polypyrrole specimen.

PPy growth pattern on LIG is clearly shown on SEM images (see Figure 6). In case of short-term deposition, typical thickening composed of polymer appear on the LIG walls. After long-term PPy deposition during 20 minutes, whole LIG surface gets coated with large PPy globules and isolated PPy bulk phase appears, therefore specific capacitance related to the PPy weight is reduced considerably. It shall be added that PPy application to the LIG surface causes considerable complication of the Raman spectrum of the test specimen (see Figure 7). The Raman spectrum of the PPy-modified LIG film has additional bands with 930, 1045, 1075, 1250, 1370, 1465 cm^{-1} frequency shifts corresponding to the bands of conducting PPy forms (cation radicals and bipolarons) [41]. In this case, it should be noted that Raman bands of PPy and LIG carbon bonds (1200–1620 cm^{-1}) overlap.

Increased LIG thickness enables considerable increase in the number of deposited PPy in pore space and LIG

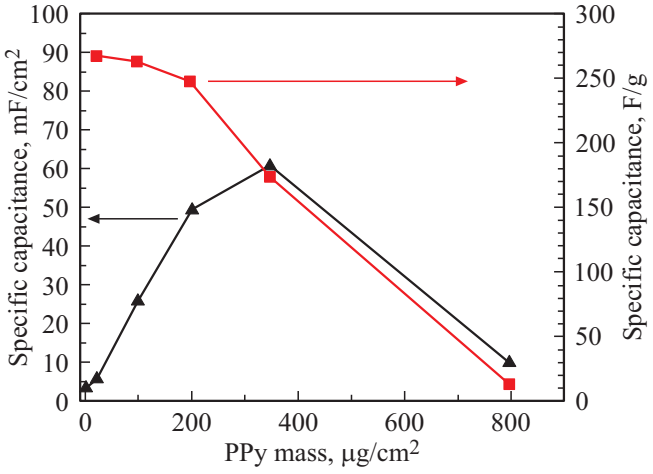

Figure 5. LIG specific capacitance dependence on the amount of electro-deposited PPy based on the geometric surface area of the LIG (left scale, solid line with triangles) and weight of electro-deposited PPy weight (right scale, line with squares).

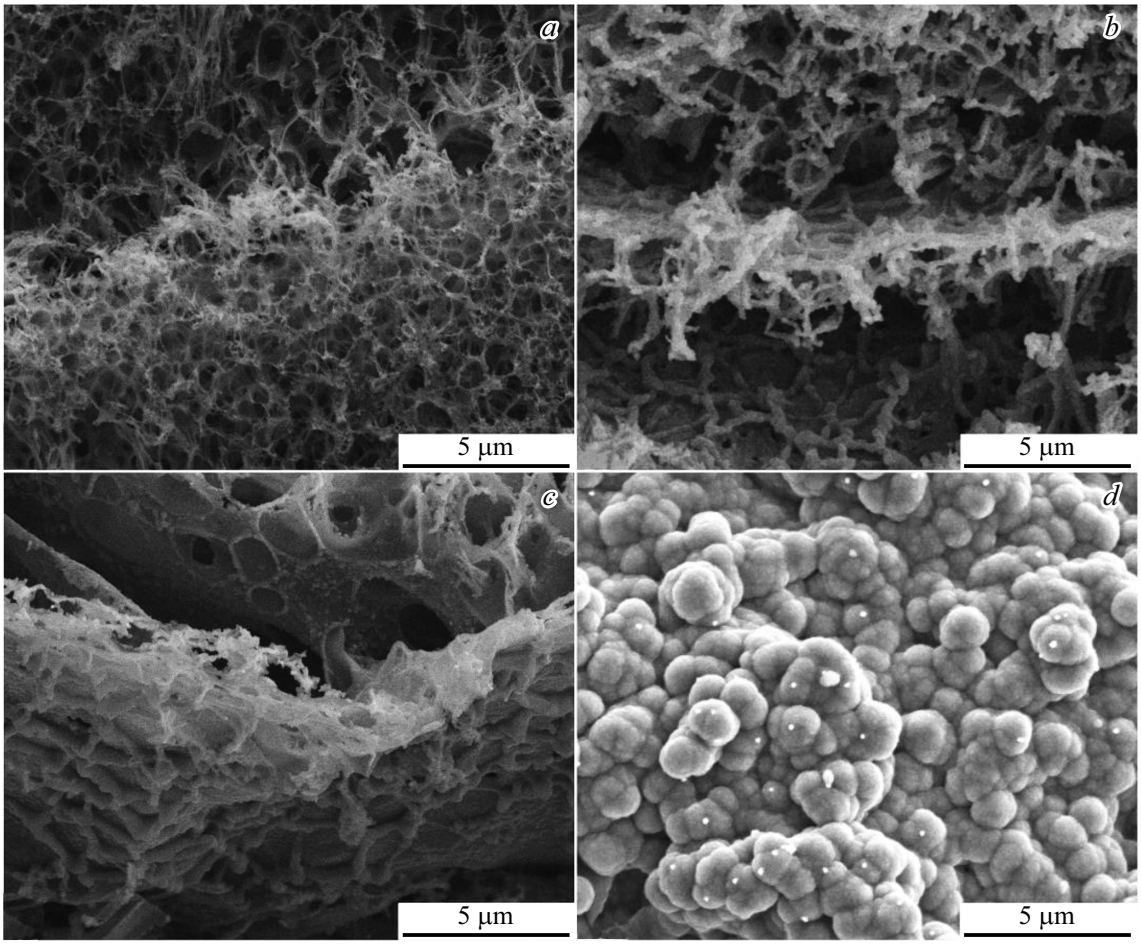

Figure 6. SEM images of LIG surface after PPy deposition on the surface within (*a*) 1, (*b*) 5, (*c*) 10 and (*d*) 20 minutes.

capacitance growth. For example, [42] describes a special chemical synthesis of films from polyamic acid which is used as polyimide precursor. Laser treatment of such specially synthesized film allowed to form a rather thick LIG layer (more than 300 μm). Long-term PPy deposition in such LIG helped to achieve very high values of capacitance ($\sim$ 2400 mF/cm^2). This research is focused on LIG which can be easily produced on the available commercial polyimide film without any special synthesis.

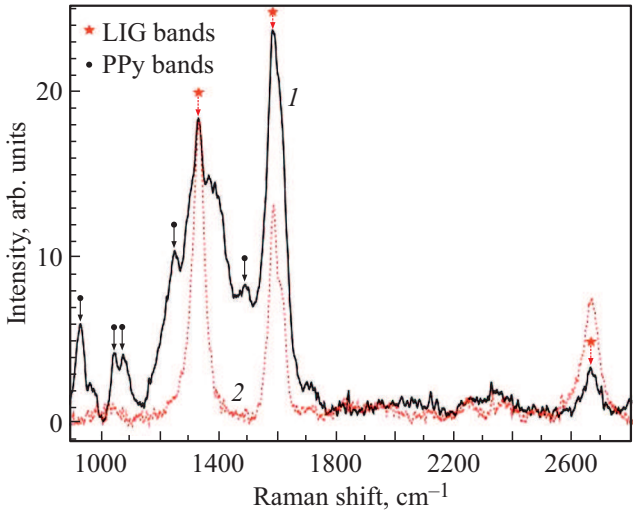

Figure 7. Raman spectra of LIG specimens: (*1*) PPy-modified during 1 minute, and (*2*) without modification.

Maximum specific capacitances for PPy-modified specimen on a commercial film are more moderate and are equal to 50–60 mF/cm^2 at the optimum amount of polymer per 1 cm^2 of the visible surface equal to 200–350 μg (see Figure 5). Thus, PPy electrodeposition on LIG synthesized on the commercial polyimide film surface allows to increase capacitance by approximately a factor of 15.

When addressing other modification versions of porous LIG structure, good results can be achieved for substances featuring maximum specific capacitance and the highest density required for maximum loading of the porous space without isolation. Hence, it may be useful to use modification with polyaniline whose specific capacitance is ($\sim$ 550 mF/cm^2) [43,44], which is $\sim$ 2 times higher that of PPy, and density is a little lower (1.33 g/cm^3 compared with 1.60 g/cm^3 for PPy). Hence, specific capacitance higher than 100 mF/cm^2 can be achieved for polyaniline-modified

LIG. Transition metal oxides (MnO_2, Fe_2O_3) whose density is much higher ($\sim 5\,g/cm^3$) than that of polymers offer promising potential to be used as modifiers.

PPy-modified LIG films were used to make a hydrogel capacitor mockup based on sulfuric acid and PVA using the aforesaid scheme. Two-electrode measurements have shown that capacitance of the produced capacitor mockup was 230 mF at the specific capacitance per unit surface of about $29\,mF/cm^2$.

4. Conclusion

Thus, line-by-line scanning of focused continuous CO_2 laser beam on the polyimide film surface makes it possible to form a porous carbon film surface structure whose thickness is up to several tens of micrometers. The recorded Raman spectra in various points in depth show that graphene structure is formed primarily on the LIG surface and the synthesized material near the polyimide interface consists of amorphous carbon. It has been demonstrated that the specific capacitance of LIG depended on the synthesis conditions (laser power, line spacing) and may be many times greater due to modification with redox-active conducting polymer. It has been found that there was an optimum amount of electrodeposited PPy where the specific capacitance of the LIG film structure achieves its maximum value. Deposition of a high amount of PPy results in porous space occlusion and isolation and sharp capacitance decrease. It has been demonstrated that PPy-modified LIG films can be used to make MSC with hydrogel electrolyte whose specific capacitance is $29\,mF/cm^2$.

Funding

This study was supported by grant No. 22-72-00017 provided by the Russian Science Foundation (https://rscf.ru/project/22-72-00017/). The experiments have been carried out using the equipment provided by the Shared Use Center „Center of Physical and Physicochemical Methods of Analysis and Study of the Properties and Surface Characteristics of Nanostructures, Materials, and Products“ of the Udmurt Federal Research Center, Ural Branch of RAS.

Conflict of interest

The authors declare that they have no conflict of interest.

References

[1] Y. Bleu, F. Bourquard, T. Tite, A.-S. Loir, C. Maddi. Front. Chem. **6** (2018).
[2] V.B. Mohan, K. tak Lau, D. Hui, D. Bhattacharyya, V. Balaji, K. tak Lau, D. Hui, D. Bhattacharyya. Compos. Part B Eng. **142**, 200 (2018).
[3] H. Tan, D. Wang, Y. Guo. Coatings **8**, 40 (2018).
[4] A. Adetayo, D. Runsewe. Open J. Compos. Mater. **9**, 207 (2019).
[5] A. Hussain, S. Muntazir, N. Abbas, M. Hussain, R. Ali. Mater. Chem. Phys. **248**, 122924 (2020).
[6] J. Lin, Z. Peng, Y. Liu, F. Ruiz-Zepeda, R. Ye, E.L.G.G. Samuel, M.J. Yacaman, B.I. Yakobson, J.M. Tour. Nature Commun. **5**, 5714 (2014).
[7] A. Lamberti, F. Perrucci, M. Caprioli, M. Serrapede, M. Fontana, S. Bianco, S. Ferrero, E. Tresso. Nanotechnology **28**, 174002 (2017).
[8] L.X. Duy, Z. Peng, Y. Li, J. Zhang, Y. Ji, J.M. Tour. Carbon **126**, 472 (2018).
[9] J.B. In, B. Hsia, J.-H. Yoo, J.-H. Yoo, S. Hyun, C. Carraro, R. Maboudian, C.P. Grigoropoulos. Carbon **83**, 144 (2015).
[10] J. Cai, C. Lv, A. Watanabe. J. Mater. Chem. A **4**, 1671 (2016).
[12] B. Kulyk, B.F.R. Silva, A.F. Carvalho, P. Barbosa, A.V. Girão, J. Deuermeier, A.J.S. Fernandes, F.M.L. Figueiredo, E. Fortunato, F.M. Costa. Adv. Mater. Technol. **2022**, 2101311 (2022).
[13] F. Wang, K. Wang, B. Zheng, X. Dong, X. Mei, J. Lv, W. Duan, W. Wang, Mater. Technol. **33**, 340 (2018).
[14] R. Ye, D.K. James, J.M. Tour. Acc. Chem. Res. **51**, 1609 (2018).
[15] Y. Chyan, R. Ye, Y. Li, S.P. Singh, C. J. Arnusch, J.M. Tour. ACS Nano **12**, 2176 (2018).
[16] K.G. Mikheev, R.G. Zonov, T.N. Mogileva, A.E. Fateev, G.M. Mikheev, Opt. Laser Technol. **141**, 107143 (2021).
[17] C.T. Long, J.H. Oh, A.D. Martinez, C.I. Sanchez, A. Sarmah, K. Arole, M.T. Rubio, M.J. Green. Carbon **200**, 264 (2022).
[18] K.G. Mikheev, R.G. Zonov, A.V. Syugaev, D.L. Bulatov, G.M. Mikheev. PSS, **64**, 579 (2022).
[19] Y. Li, D. X. Luong, J. Zhang, Y. R. Tarkunde, C. Kittrell, F. Sargunaraj, Y. Ji, C.J. Arnusch, J.M. Tour. Adv. Mater. **29**, 1700496 (2017).
[20] H. Wang, Z. Zhao, P. Liu, X. Guo. Biosensors **12**, 55 (2022).
[21] P. Xue, Z. Huang, C. Chen. Lubricants **10**, 239 (2022).
[22] R. Ye, D.K. James, J.M. Tour. Adv. Mater. **31**, 1803621 (2019).
[23] L. Lan, X. Le, H. Dong, J. Xie, Y. Ying, J. Ping. Biosens. Bioelectron. **165**, 112360 (2020).
[24] Y.H. Yen, C.S. Hsu, Z.Y. Lei, H.J. Wang, C.Y. Su, C.L. Dai, Y.C. Tsai. Micromachines **13**, 1 (2022).
[25] Y.P. Suhorukov, A.V. Telegin, K.G. Mikheev, R.G. Zonov, L.I. Naumova, G. M. Mikheev. Opt. Mater. **133**, 112957 (2022).
[26] J. Liu, H. Ji, X. Lv, C. Zeng, H. Li, F. Li, B. Qu, F. Cui, Q. Zhou. Microchim. Acta **189**, 54 (2022).
[27] J. Gao, S. He, A. Nag. Sensors **21**, 2818 (2021).
[28] K.G. Mikheev, R.G. Zonov, D.L. Bulatov, A.E. Fateev, G.M. Mikheev. Tech. Phys. Lett. **46**, 458 (2020).
[29] E.L. Ivchenko. Phys. Status Solidi **249**, 2538 (2012).
[30] A.S. Saushin, G.M. Mikheev, V.V. Vanyukov, Y.P. Svirko. Nanomaterials **11**, 2827 (2021).
[31] C. Zhang, W. Lv, Y. Tao, Q.-H. Yang. Energy Environ. Sci. **8**, 1390 (2015).
[32] N.A. Kyeremateng, T. Brousse, D. Pech. Nat. Nanotechnol. **12**, 7 (2017).
[33] M. Beidaghi, Y. Gogotsi. Energy Environ. Sci. **7**, 867 (2014).
[34] J. Bae, M.K. Song, Y.J. Park, J.M. Kim, M. Liu, Z.L. Wang, Angew. Chem. Int. Ed. **50**, 1683 (2011).
[35] Z. Peng, R. Ye, J.A. Mann, D. Zakhidov, Y. Li, P.R. Smalley, J. Lin, J.M. Tour. ACS Nano **9**, 5868 (2015).

[36] L. Li, J. Zhang, Z. Peng, Y. Li, C. Gao, Y. Ji, R. Ye, N.D. Kim, Q. Zhong, Y. Yang, H. Fei, G. Ruan, J.M. Tour. Adv. Mater. **28**, 838 (2016).
[37] A.C. Ferrari. Solid State Commun. **143**, 47 (2007).
[38] A.C. Ferrari, J.C. Meyer, V. Scardaci, C. Casiraghi, M. Lazzeri, F. Mauri, S. Piscanec, D. Jiang, K.S. Novoselov, S. Roth, A.K. Geim. Phys. Rev. Lett. **97**, 1 (2006).
[39] L.M. Malard, M.A. Pimenta, G. Dresselhaus, M.S. Dresselhaus. Phys. Rep. **473**, 51 (2009).
[40] A. Kaidarova, J. Kosel. IEEE Sens. J. *21*, 12426 (2021).
[41] Y. Furukawa, S. Tazawa, Y. Fujii, I. Harada. Synth. Met. **24**, 329 (1988).
[42] X. Yu, N. Li, S. Zhang, C. Liu, L. Chen, S. Han, Y. Song, M. Han, Z. Wang, J. Power Sources **478**, 229075 (2020).
[43] S.R. Sivakkumar, W.J. Kim, J. A. Choi, D.R. MacFarlane, M. Forsyth, D.W. Kim. J. Power Sources **171**, 1062 (2007).
[44] N. Mahato, D. Mohapatra, M.H. Cho, K.S. Ahn. Energies **15**, 2001 (2022).

Translated by Ego Translating